



Decomposition of antibiotic ornidazole by gamma irradiation in aqueous solution: kinetics and its removal mechanism

Rahil Changotra¹ · Jhimli Paul Guin² · Amit Dhir¹ · Lalit Varshney²

Received: 3 May 2018 / Accepted: 16 August 2018 / Published online: 21 September 2018
© Springer-Verlag GmbH Germany, part of Springer Nature 2018

Abstract

An efficient gamma radiolytic decomposition of one of the extensively used pharmaceutical ornidazole (ORZ) was explored under different experimental conditions by varying initial concentrations, solution pHs, and doses and concentrations of inorganic (CO_3^{2-}) and organic (*t*-BuOH) additives. The results showed that low ORZ concentrations could be efficiently decomposed using gamma irradiation. The decomposition was followed by pseudo first-order reaction kinetics with rate constant values of 2.34, 1.48, 1.11, and 0.80 kGy^{-1} for the following initial concentrations: 25, 50, 75, and 100 mg L^{-1} with their corresponding ($G(-\text{ORZ})$) values of 1.004, 1.683, 2.237, and 2.273, respectively. Decomposition rate of ORZ was remarkably improved under acidic condition when compared to neutral or alkaline medium. It was also observed that the decomposition was primarily caused by the reaction of ORZ with radiolytically generated reactive HO^\bullet radicals. The addition of H_2O_2 had a synergistic effect on the decomposition and mineralization extent of ORZ. However, the removal of total organic carbon (TOC) was not as effective as the decomposition of ORZ. Finally, the quantum chemical calculations were employed to optimize the geometry structure of ORZ and liquid chromatography quadrupole time-of-flight mass spectrometry (LC-QTOF-MS) was used to identify the decomposition intermediates. On the basis of Gaussian calculations and analysis of LC-QTOF-MS, it can be inferred that ORZ radiolytic decomposition was mainly attributed to oxidative HO^\bullet radicals and the direct cleavage of ORZ molecules. Possible pathways for ORZ decomposition using gamma irradiation in aqueous medium were proposed.

Keywords Gamma irradiation · Ornidazole · Decomposition · Kinetics · Gaussian calculation · Removal pathways

Introduction

Occurrence of pharmaceutical contaminants in the environment has lifted plenteous contemplation owing to their potential ecological and environmental impacts (Schwarzenbach

et al. 2006; Kumar and Xagorarakis 2010). Antibiotics are among one of the most important and extensively used class of pharmaceuticals in today's medicine which may intrude into the environment as parent compounds or metabolites after being excreted (Sánchez-Polo et al. 2009). Ornidazole (ORZ) is a profusely utilized pharmaceutical drug for human and veterinary treatment (Zhao et al. 2012). Due to its antibacterial/antiprotozoal properties, ORZ has been widely used for the treatment of trichomoniasis, giardiasis (lambliasis), genitourinary infections, bacterial vaginosis, trichomoniasis (Khattab et al. 2012). Available literature suggests that within 5 days of consumption of a single ORZ oral dose, 85% fraction is discharged from the body with corresponding 63% via urine and remaining 22% fraction in the feces (Schwartz and Jeunet 1976; Solomon et al. 2008). Continuous input of ORZ leads to chronic low-level environmental risk, inflation, and may induce unfavorable effects on ecosystems and life (Changotra et al. 2018a).

Due to the high endurance towards conventional biodegradation, pharmaceuticals have been intermittently detected in

Responsible editor: Ester Heath

Electronic supplementary material The online version of this article (<https://doi.org/10.1007/s11356-018-3007-x>) contains supplementary material, which is available to authorized users.

✉ Jhimli Paul Guin
jhpaul@barc.gov.in

✉ Amit Dhir
amit.dhir@thapar.edu

¹ School of Energy and Environment, Thapar Institute of Engineering and Technology, Patiala -147004, India

² Radiation Technology Development Division, Bhabha Atomic Research Centre, Trombay, Mumbai -400085, India

drinking water (Andreozzi et al. 2006; Schaidler et al. 2014); surface water (Dinh et al. 2011; Henzler et al. 2014; Shanmugam et al. 2014; Changotra et al. 2017); wastewater (Nam et al. 2014; Kostich et al. 2014); and sediments (Chen and Zhou 2014). Studies showed that biological treatments were inept in degrading and eliminating genotoxicity of clinically important antibiotics. A combined aerobic and anaerobic treatment system utilized for the treatment of high-strength pharmaceutical wastewater was found efficient in reducing chemical oxygen demand (COD), but was incompetent towards antibiotic removal (Kümmerer et al. 2000). The sewage treatment plants are ineffective in degrading these compounds, thereby increasing the organic load of the treated wastewater, which becomes non-recyclable. Therefore, discharging the wastewater to the main water stream also adversely affects the ecosystem of aquatic environment (Watkinson et al. 2007; Le-Minh et al. 2010). Moreover, the photo and thermal stability of ORZ in natural aqueous environment demand to find an effective treatment method for efficient decomposition of such pollutant in order to enhance recyclability of wastewaters as well as to reduce the adverse impacts on environment (Singh et al. 2003; Puttaswamy and Shubha 2009; Zhao et al. 2012).

As an alternative to conventional methods, advanced oxidation processes (AOPs) such as photocatalysis, fenton, and ozonation have been proven eminently robust for the decomposition of numerous types of organic pharmaceutical pollutants due to their ability to produce non-selective and highly reactive species such as hydroxyl radical (HO^\bullet). These reactive species react with the high molecular weight contaminant and are able to degrade it into low molecular weight by-products, or even attaining their complete mineralization (Dantas et al. 2008; Zhao et al. 2012; Panizza et al. 2014; Tayo et al. 2018). On the other hand, toxicity of selective by-products, higher treatment cost, dependence on the surface properties of the photocatalyst based on the composition of wastewater and lesser mineralization extents of the intermediate products formed by these AOPs limit their practical application (Hapeshi et al. 2010; Michael et al. 2010; Guin et al. 2014; Guin et al. 2014a; Tay and Madehi 2015). However, from literature review, it is obvious that limited studies are available on the decomposition of aqueous solution of ORZ by the application of AOPs. Puttaswamy and Shubha (2009) demonstrated the extent of decomposition of ORZ in Ruthenium (III) - Osmium (VIII) - catalyzed oxidation reaction system. On the other hand, Zhao et al. (2012) evaluated the decomposition efficiency of ORZ in presence of visible light-activated Y^{3+} - $\text{Bi}_5\text{Nb}_3\text{O}_{15}$ catalyst. However, these methods either generated the secondary pollution during the treatment processes or showed relatively low removal efficiency with high cost of treatment.

As an advanced oxidation process, gamma radiolysis is considered as a promising treatment option which has been

extensively used for the decomposition of wide variety of stable organic pollutants including, herbicides (Bojanowska-Czajka et al. 2006), pesticides (Mohamed et al. 2009), nitroaromatic compounds (Bao et al. 2009; Basfar et al. 2009), and pharmaceuticals (Razavi et al. 2009; Liu et al. 2011; Liu et al. 2015; Khan et al. 2015; Sayed et al. 2016; Guo et al. 2017; Kim et al. 2017). Easier operation, least requirement of additional chemicals, minimum production of toxic intermediates, devoid of any sludge production, insensitive to suspended solids and color in the wastewater are few advantages of high energy radiation technology (Cantwell and Hofmann 2011; Paul et al. 2014; Borrelly et al. 2016; Liu et al. 2018; Changotra et al. 2018). Earlier investigations revealed the significant role of radiation technology on improving the treatment efficiency of sewage, paper mill and textile dye effluent (Paul et al. 2013). Radiation-based dye effluent and sludge treatment plants were also established nationally and internationally. Therefore, radiation technology could also play a prominent role in near future in pilot as well as commercial scale to treat real pharmaceutical effluent.

Literature analysis showed that radiolytic decomposition of aqueous solution of ORZ was rarely investigated. Therefore, the present study was aimed to assess the effect of gamma radiation on ORZ decomposition for the first time. Effect of various reaction parameters such as initial concentrations of ORZ, oxidant, doses, and solution pHs were judiciously optimized in order to obtain best radiolytic decomposition efficiency of ORZ. The decomposition kinetics of ORZ under different reaction conditions and in presence of oxidant was thoroughly monitored to demonstrate viability of radiolytic decomposition of ORZ in aqueous medium. The probable reaction routes and decomposition products were analyzed in order to understand the insight decomposition mechanism of ORZ.

Experimental

Chemicals and reagents

Ornidazole (purity $\geq 99\%$), *tert*-Butanol and HPLC grade acetonitrile (purity $\geq 99.9\%$) were procured from Sigma-Aldrich. Hydrogen peroxide 30% (*w/v*), sodium hydroxide ($> 99\%$), hydrochloric acid (37%), and phosphoric acid (88%) were analytic grade reagents with high purity obtained from Merck. Sodium carbonate (purity $> 99\%$) was purchased from TCI Chemicals. The culture media, Muller Hinton Agar (MHA) was procured from Himedia. The microbes, *Escherichia coli* (DH5- α strain), *Bacillus subtilis* (MTCC 441), and *Pseudomonas aeruginosa* (MTCC 647), were obtained from the Department of Biotechnology, Thapar Institute of Engineering and Technology, Patiala (Punjab).

Ultrapure water from Milli-Q system was used throughout the experimental work.

Experimental

Aqueous solutions of ORZ were permitted to attain state of equilibrium under room temperature and atmospheric pressure prior to radiation exposure and were tightly closed in order to prevent the introduction of air. Irradiation studies were performed in a GC-5000 gamma chamber having ^{60}Co as a source of gamma radiation. The dose rate was found to be 0.75 kGy h^{-1} as determined by means of Fricke dosimetry [$G(\text{Fe}^{3+}) = 1.61 \mu\text{m/J}$]. Aqueous solutions of ORZ with different initial concentrations (25, 50, 75, and 100 mg L^{-1}) were irradiated at different doses in a 30-mL air-tight borosilicate glass vials loaded with 20 mL solution at different doses in presence of Na_2CO_3 , *t*-BuOH, and H_2O_2 . The pH values of the solutions were adjusted using 1 M HCl and 1 M NaOH. The glass container with solutions was placed inside a closed lead-shielded gamma source with the aid of an electronically controlled motorized stage ensuring the safety of the operator. The irradiation with gamma energy 1.25 MeV was carried out in non-contact mode. It does not induce radioactivity to the ORZ composed of low atomic number elements like C, H, and N and hence does not promote any health hazards (Spinks and Woods 1990). After gamma radiolysis of ORZ solution at a specified dose (the irradiation time was calculated with the quotient of specified dose and dose rate), the irradiated samples were preserved in refrigerator at $4 \text{ }^\circ\text{C}$ until further analysis.

Analytical techniques

The concentration of ORZ in aqueous medium was examined using high-performance liquid chromatography (HPLC 20AD, Shimadzu Corporation, Japan) which was equipped with C_{18} reversed-phase column (Enable C18G ($250 \times 4.6 \text{ mm}$; $5 \mu\text{m}$)) and diode array detector (SPD-M20A). The elution was carried out with mobile phase of water and acetonitrile (60:40, *v/v*) at 1 mL min^{-1} flow rate; and with detection of ORZ at 320 nm. A fixed volume injection loop was used to inject $20 \mu\text{L}$ of sample for every determination. Typically, the retention time of ORZ was 5.35 min under these conditions. In order to validate the stability of the system, linear standard calibration curves with four or five point were plotted regularly during the analysis period.

TOC analyzer (multi N/C 2100, AJ Analytikjena, Germany) was used to estimate the mineralization efficiency in terms of total organic carbon (TOC) content of irradiated samples. pH of ORZ solution was measured by Cyber Scan PCD 650 multiparameter analyzer.

The identification of ORZ and its intermediate products were characterized by using liquid chromatography

quadrupole time-of-flight mass spectrometer (LC-QTOF/MS, Micromass Q-TOF micro, Waters, USA) equipped with Unisol YVR C_{18} reverse-phased column and separation module (Waters Alliance 2795). The sample injection volume was $20 \mu\text{L}$ and similar mobile phase conditions were utilized as used in the analysis of ORZ in HPLC system. The ESI-MS analysis was executed in positive mode using electro spray ionization source with source temperature at $110 \text{ }^\circ\text{C}$ and spray voltage of 3000 V. Nitrogen was used as sheath gas with flow rate of 30 L hr^{-1} and pressure of 6–7 bar. The full scan mode was used to acquire spectrum over the mass range 60–400 *m/z* and other parameters were as follows: 550 L h^{-1} desolvation gas flow rate; $300 \text{ }^\circ\text{C}$ desolvation temperature; $110 \text{ }^\circ\text{C}$ source temperature; and 3 kV capillary voltage. Cytotoxicity potential of ORZ and its irradiated solutions was examined through Standard Kirby-Bauer (disk diffusion method) against clinical isolates of three microbes: *E. coli*, *B. subtilis*, and *P. aeruginosa* and same procedure was followed as reported in the study (Changotha et al. 2018). Statistical significance of the experiment results were analyzed using one-way analysis of variance (ANOVA) test with the aid of GraphPad Prism Software Version 5.01.

Radiation-chemicals yield (G(-ORZ)) and dose constants calculation

The decomposition extent of ORZ is usually expressed in the terms of radiation-chemical yields ($G(-\text{ORZ})$) values, using Eq. 1. (Spinks and Woods 1990; Woods and Pikaev 1994):

$$G = \frac{A (6.023 \times 10^{23})}{D (6.24 \times 10^{16})} \quad (1)$$

where A is the change in the concentration of ORZ (M); 6.023×10^{23} is Avogadro's number; D is absorbed dose (Gy); and 6.24×10^{16} is the Gy to 100 eV L^{-1} conversion factor.

The dose constant (k) was determined using slope of the plot of natural logarithm [\ln] of ORZ concentration against absorbed dose (kGy). The dose constants values were utilized to determine the required dose to decompose 50% ($D_{0.50}$) and 90% ($D_{0.90}$) ORZ by the Eqs. (2) and (3).

$$D_{0.50} = \ln 2/k \quad (2)$$

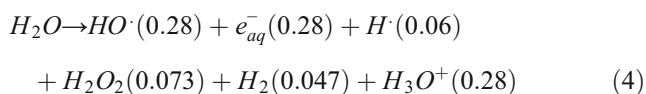
$$D_{0.90} = \ln 10/k \quad (3)$$

Results and discussion

Radiolytic decomposition of ORZ

The gamma radiolytic decomposition of aqueous solution of ORZ at different initial concentrations was investigated

(Fig. 1a). It was observed from the figure that extent of decomposition of ORZ was increased with increase in an absorbed dose for a particular concentration of the compound. 99.2 and 99% of decompositions were achieved at dose of 3.0 kGy with the initial concentrations (ORZ) of 25 and 50 mg L⁻¹, respectively. However, the decomposition of ORZ decreased with increasing initial concentrations with the dose. At an absorbed dose of 1.0 kGy, 91.5, 75.9, 58.7, and 51.5% of ORZ decomposition were achieved at the initial concentrations of 25, 50, 75, and 100 mg L⁻¹, respectively. The degradation of ORZ was found to be negligible under control experiment carried out at room temperature in absence of gamma radiation. Moreover, the decomposition extent (removal (%)) of 50 mg L⁻¹ ORZ was also compared with calculated (*G*(-ORZ)) values (Fig. 2). The inset of Fig. 2 shows the pattern of absorption spectra of irradiated ORZ solutions. The intensities in the characteristic absorption peaks of ORZ at 320 nm and 232 nm were decreased with increase in the doses owing to the removal of the compound. Further, the (*G*(-ORZ)) values for the radiolytic decomposition of ORZ were calculated to be 1.68 and 0.72 for an absorbed doses of 1.0 and 3.0 kGy, respectively. Results revealed a decrease in (*G*(-ORZ)) value and an increase in decomposition of ORZ with the increasing absorbed doses. Gamma radiolytic decomposition of the organic pollutants in aqueous solution is initiated by the reaction with the reactive radicals (HO[•], e_{aq}⁻, and H[•]) produced during the gamma radiolysis of water as mentioned in Eq. 4 (Woods and Pikaev 1994).



where the numbers in parentheses indicate the radiation chemical yield of species production (*G* value) in μmol J⁻¹. However, the decrease in (*G*(-ORZ)) with the increase in absorbed doses is attributed due to the increase in probability of competition reactions between ORZ and decomposed products of ORZ molecules for reacting with the reactive radical species produced during water radiolysis in Eq. 4 (Basfar et al. 2005; Sánchez-Polo et al. 2009). Moreover, radical-radical

Fig. 1 Radiolytic decomposition of different concentration of ORZ against absorbed dose (a) and the pseudo-first-order kinetics of ORZ decomposition (b)

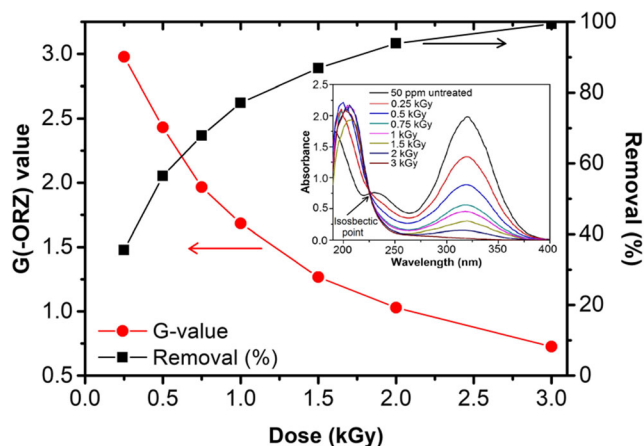
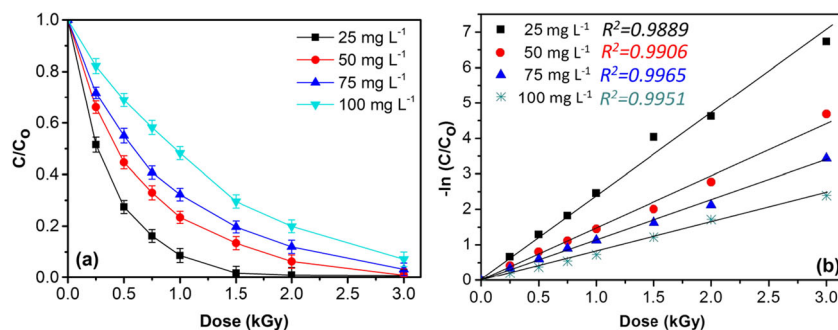


Fig. 2 *G* values versus percent removal of ORZ using gamma irradiation. [(ORZ)₀ = 50 mg L⁻¹; pH = 6.5] (inset: absorption spectrum of ORZ at 190–400 nm after irradiation treatment)

recombination reaction during radiolysis also leads to a decrease in (*G*(-ORZ)) values with doses (Liu et al. 2011). The increases in the absorption of ORZ with increase in absorbed dose in the wavelength range of 190–230 nm also signifies the generation of reaction by-products or intermediates as evidenced from inset of Fig. 2 (Chu et al. 2016; Huang et al. 2016). Further, the appearance of isosbestic point at 246 nm indicates the generation and accumulation of intermediates during the radiolytic decomposition of ORZ (Tian et al. 2009; el mehdi Benacherine et al. 2017). However, an enhancement in the increase in total amount of reactive radicals in solution with increase in accumulated absorbed dose leads to increase the overall decomposition extent of ORZ at each dose.

From Fig. 1b, it was evident that ORZ concentration was decreased exponentially with the increase in absorbed dose. This is represented by Eq. 5, which is in agreement with the pseudo first-order-rate kinetics.

$$-\ln(C/C_0) = Dk \quad (5)$$

where *C* is residual concentration of ORZ after irradiation treatment, *C*₀ is the ORZ concentration before irradiation treatment, *D* is the irradiation absorbed dose (kGy), and *k* is the dose constant of ORZ decomposition (kGy⁻¹), which

could be effected by the several experimental conditions such as, solution pH, chemical structure of organic contaminant, initial concentration of organic contaminant, and the characteristics of solvent and/or additive used. Therefore, in this study, the decomposition rate of ORZ at different initial concentrations could be well-fitted to Eq. 5 to calculate dose constants.

The corresponding dose constants are shown in Table 1. Interestingly, the decrease in *k* value from 2.340 to 0.806 kGy⁻¹ for the initial ORZ concentration of 25 to 100 mg L⁻¹ were observed which showed the significant dependence of initial concentration on the corresponding dose constant. The decrease in *k* value with increased initial concentration of ORZ was resulted due to simultaneous competition reactions of ORZ and its decomposition intermediates with the radiolytically generated reactive radicals (Magureanu et al. 2010). The dose constant, *k*, was taken into account to determine the dose required to bring about 50% (*D*_{0.50} values) and 90% (*D*_{0.90} values) decomposition of ORZ as calculated by Eqs. 2 and 3 and the results obtained are shown in Table 1. These results also signify that, at lower *C*₀ of ORZ, lower dose was required to obtain 50% and 90% decomposition extents of ORZ with correspondingly higher dose constant values and vice versa.

Effect of solution pH

Figure 3 represents the influence of solution pH on gamma radiolytic decomposition of ORZ. It was found that the ORZ decomposition efficiency was higher in the acidic medium when compared to alkaline and neutral medium. With

1.0 kGy of an absorbed dose, ORZ decomposition efficiency was found to be 75, 70.1, and 66.3% at the pH of 3, 6.5, and 11 with the corresponding *k* values of 1.631, 1.260, and 0.995 kGy⁻¹, respectively (Table 1, experiments 5–7).

The *pK_a* of ORZ was reported as 2.4 and thus ORZ was expected to in its molecular form in the studied pH range (Salo et al. 2003). The decomposition rate of pollutant during gamma radiolysis explicitly depends upon the existing radical species (Guo et al. 2015; Liu et al. 2015). It is understood that pH of the solution influences the yield of key reactive species during water radiolysis and hence affects the decomposition efficiency of ORZ. In acidic solution (pH 3.0), fraction of *e_{aq}⁻* is converted into H[•] on reaction with H⁺ (2.3×10^{10} L mol⁻¹ s⁻¹) (Guo et al. 2012). The reduced *e_{aq}⁻* concentration confines its reaction with HO[•] to form OH⁻, thus increases relative concentration of HO[•] radical (*G* value = 0.28 μmol J⁻¹) in the aqueous medium to react with ORZ molecules (Spinks and Woods 1990; Zheng et al. 2011). Thus, HO[•] is expected to initiate the decomposition of ORZ via formation of ORZ epoxide. It degrades into 2-methyl-5-nitroimidazole through subsequent cleavage of epoxide ring followed by demethylation (Zhao et al. 2012). Overall reaction increases the decomposition efficiency of ORZ. On the other hand, in alkaline solution (pH 11.0), fraction of HO[•] radical (*pK_a* = 11.9) reacts with OH⁻ ions to produce weak oxidative O⁻ species and H₂O (1.30×10^{10} L mol⁻¹ s⁻¹). Thus, it decreases the concentration of HO[•] (*G* value < 0.28 μmol J⁻¹) in the aqueous medium as well as decomposition efficiency of ORZ (Basfar et al. 2005). Similar trend in results were also observed in the published reports (Sayed et al. 2016; Chu et al. 2016; Changotra et al. 2018). From

Table 1 Data from gamma radiolytic experiments of ORZ: influence of initial concentration, pH, and various additives. [*G* value calculated for 1 kGy dose using Eq. 1]

Exp.	[ORZ] ₀ (mg L ⁻¹)	pH	[Na ₂ CO ₃] (M)	[<i>t</i> -BuOH] (M)	[H ₂ O ₂] (mM)	<i>G</i> value	<i>k</i> (kGy ⁻¹)	<i>D</i> _{0.5} (kGy)	<i>D</i> _{0.9} (kGy)
1	25	6.5	0	0	0	1.004	2.340	0.296	0.983
2	50	6.5	0	0	0	1.683	1.483	0.467	1.552
3	75	6.5	0	0	0	2.237	1.119	0.619	2.057
4	100	6.5	0	0	0	2.273	0.806	0.859	2.856
5	50	3	0	0	0	1.724	1.631	0.424	1.411
6	50	6.5	0	0	0	1.627	1.260	0.547	1.818
7	50	11	0	0	0	1.464	0.995	0.696	2.314
8	50	6.5	0.05	0	0	1.190	0.650	1.066	3.542
9	50	6.5	0.1	0	0	0.990	0.482	1.438	4.777
10	50	6.5	0	0.05	0	0.345	0.186	3.726	12.37
11	50	6.5	0	0.1	0	0.215	0.123	5.635	18.72
12	50	6.5	0	0	0.5	1.884	1.970	0.351	1.168
13	50	6.5	0	0	5	2.009	2.234	0.310	1.030
14	50	6.5	0	0	10	1.987	1.730	0.400	1.330
15	50	6.5	0	0	20	1.852	1.528	0.453	1.506

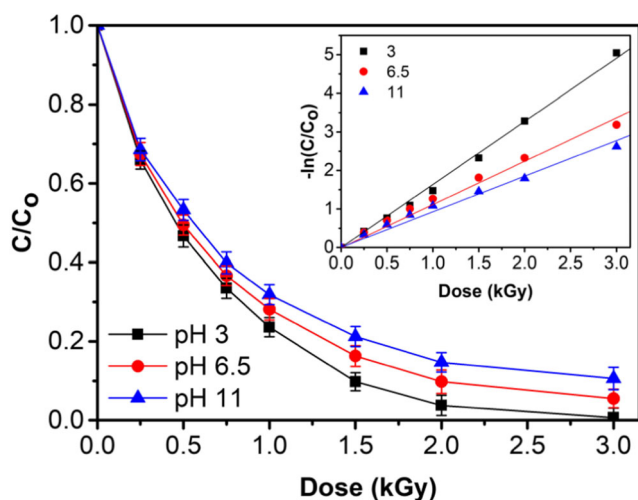


Fig. 3 Influence of solution pH on radiolytic decomposition of ORZ [(ORZ)₀ = 50 mg L⁻¹; pH = 6.5]

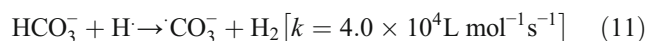
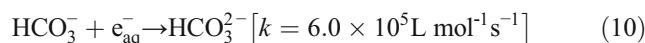
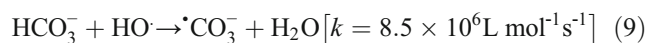
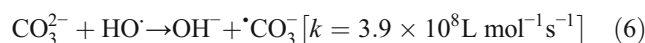
the results, it can be said that HO[•] radical play a predominant role in decomposition of aqueous solution of ORZ.

Effect of additives on ORZ radiolysis

Natural water and wastewater are considered to be complex matrices that consist of many organic and inorganic species which may retard the extent of gamma-induced radiolytic decomposition of ORZ by competing with the reactive radical species produced during gamma radiolysis. Therefore, to assess their effect on the decomposition extent of ORZ, the radiolytic decomposition efficiency of 50 mg L⁻¹ ORZ was monitored in presence of different concentrations of CO₃²⁻ and *tert*-butanol (*t*-BuOH) at pH 6.5. It can be seen from Fig. 4a, b that at a given absorbed dose, decomposition efficiency of ORZ in the solution was higher without the additives when compared to those in the presence of additives, CO₃²⁻ and *t*-BuOH. 99.4% ORZ decomposition was achieved in the aqueous solution at an absorbed dose of 3.0 kGy, while 68% and 34.5% ORZ decomposition efficiencies were obtained in the presence of 0.1 M CO₃²⁻ and *t*-BuOH, respectively. This can be attributed due to the scavenging effect of CO₃²⁻ and *t*-

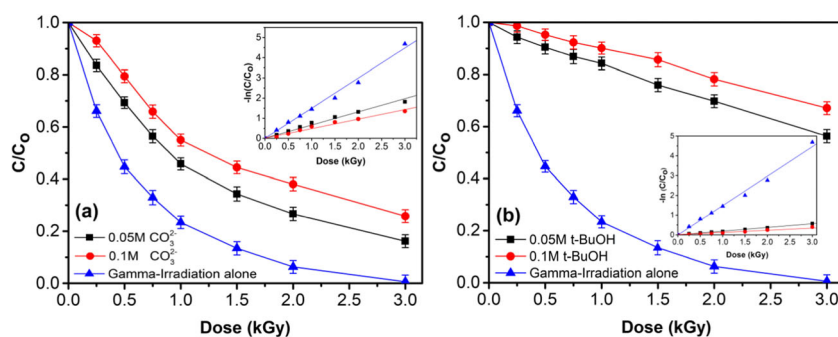
BuOH for the radical species such as HO[•], e_{aq}⁻, and H[•] as shown by Eqs. 6–14. Table 1 exhibited that the pseudo first-order reaction dose constants (*k*) for radiolytic decomposition of ORZ were decreased with increase in the concentration of CO₃²⁻ (Table 1, experiments 8–9) and *t*-BuOH (Table 1, experiments 10–11) in the aqueous solution. Moreover, the *k* values of ORZ in the presence of 0.1 M CO₃²⁻ and *t*-BuOH were found to be 0.4821 and 0.1234 kGy⁻¹, respectively which was lower than 1.483 kGy⁻¹ in the solution without the additives. Hence, the *k* value decreased with the addition of CO₃²⁻ and *t*-BuOH in the aqueous solution. It was also observed from Table 1 that the *G*(-ORZ) value was calculated to be higher in presence of CO₃²⁻ (0.990 for 0.1 M) compared to in presence of *t*-BuOH (0.215 for 0.1 M).

The preferential scavenging of HO[•] radicals by CO₃²⁻ ion leads to the formation of carbonate radical anion ([•]CO₃⁻) (Eq. 6). Although, the CO₃²⁻ ions can directly react with e_{aq}⁻, but at a much lower reaction rates (Eq. 7). It should be pointed out that the equilibrium state (Eq. 8) is established in the aqueous solution with a p*K*_a value of 10.33, accordingly, at working pH (which is < 10), the given equilibrium shifts to the left with a prevalence of HCO₃⁻ ions (Eqs. 9, 10, and 11) (Buxton et al. 1988). On the other hand, the [•]CO₃⁻ radical generated in reaction 6, 9, and 11 has a redox potential of 1.78 V at neutral pH, which can slowly oxidize ORZ (Huie et al. 1991; Hu and Wang 2007; Changotra et al. 2018).

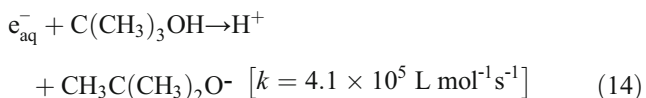
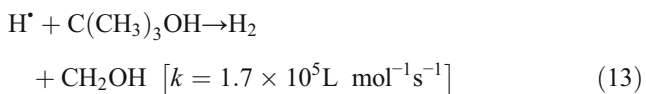
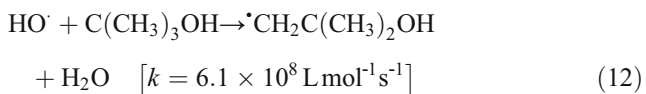


Results in Fig. 4b also demonstrated that the decomposition efficiency of ORZ with the addition of *t*-BuOH was lower than that without *t*-BuOH. Here, only 45% and 34.5% ORZ

Fig. 4 Effect of CO₃²⁻ (a) and *t*-BuOH (b) on radiolytic decomposition ORZ [(ORZ)₀ = 50 mg L⁻¹; pH = 6.5]



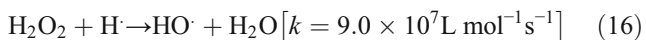
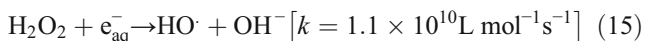
decomposition was achieved with the addition of 0.05 M and 0.1 M *t*-BuOH, respectively. *t*-BuOH could react with reactive species, which are summarized as Eqs. 12–14.



t-BuOH reacts with HO[•] radicals with moderately high rate constant (Eq. 12) (Basfar et al. 2005) and form inert radical [•]CH₂C(CH₃)₂OH. Compared to that between CO₃²⁻ and HO[•], the higher rate constant between *t*-BuOH and HO[•] results in less HO[•] radical available to react with ORZ (Eqs. 6 and 12). The lower decomposition of ORZ with *t*-BuOH than that with CO₃²⁻ suggests that HO[•] radical plays a dominant role in ORZ removal from the aqueous solution. Thus, two additives exhibit different radical reaction patterns (Eqs. 6–14), which explain the difference found in the extent of decomposition of ORZ (Table 1, experiments 8–11).

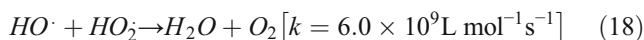
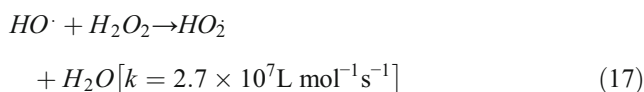
Effect of H₂O₂ on ORZ radiolysis

H₂O₂ is an HO[•] promoter and can enhance the decomposition efficiency of pollutants in the aqueous medium (Liu and Wang 2013). Figure 5 depicts the effect of H₂O₂ on the decomposition of ORZ by gamma radiolysis and the corresponding results obtained are shown in Table 1 (experiments 12–15). The results showed that the addition of concentration of 0.5 and 5 mM H₂O₂ favored ORZ decomposition with *k* values of 1.970 and 2.234 kGy⁻¹, respectively versus the *k* value (1.483 kGy⁻¹) obtained without the addition of H₂O₂ at pH 6.5 (Table 1, experiment 2). This can be explained by the fact that the rapid reaction of H₂O₂ with e_{aq}⁻ (Eq. 15) and H[•] (Eq. 16) enhances the HO[•] radical concentration in the aqueous solution and thus helped to enhance the decomposition efficiency of ORZ (Buxton et al. 1988).



However, *k* = 1.730 kGy⁻¹ was obtained with initial H₂O₂ concentration of 10 mM. It indicates that reactions 17 and 18 predominantly occur at this H₂O₂ concentration, generating less reactive peroxy radical species compared to HO[•] radical (Buxton et al. 1988). Moreover, the formed peroxy radical

species facilitates the recombination reaction with HO[•] radical (Eq. (17)) resulting a decrease in the *k* value (Table 1).



Accordingly, optimal concentration of H₂O₂ in the gamma radiolytic decomposition of ORZ was found to be 5 mM under the given experimental conditions. These results are consistent with the above section assuming that HO[•] radical is the primary species accountable for ORZ decomposition.

Mineralization study

The radiolysis treatment efficiency not only depends on the potency of radiolytic decomposition of ORZ but also on the extent of mineralization of the ORZ and its generated intermediates. Thus, the TOC removal of the irradiated aqueous solutions of ORZ at different doses was assessed to evaluate the effect of H₂O₂ on the extent of mineralization of ORZ (Fig. 6). The removal of TOC was found to be ~35% at 3.0 kGy in absence of H₂O₂. For gamma irradiation/H₂O₂ process, rather enhanced TOC removals were observed indicating that the presence of H₂O₂ had more obvious effect on mineralization of ORZ than on its decomposition. For example, it can be seen from Figs. 5 and 6, with the initial H₂O₂ concentration of 0.5, 5, 10, and 20 mM, the decomposition efficiency of ORZ was found to be 99.5, 99.7, 99.1, and 92.6% respectively; whereas, the TOC removal efficiency was found to be 34.9, 38.4, 44.0, and 57%, respectively. In the dose range of 0–3.0 kGy, TOC was removed quickly with gamma irradiation/H₂O₂ process and this trend was more obvious at initial concentration range of 5–20 mM H₂O₂. The concentration of HO[•] increases during radiolysis in presence of H₂O₂ due to the conversion of the reducing species, e_{aq}⁻ and H[•], into HO[•] (Eqs. 15 and 16). The generated HO[•], reacts non-

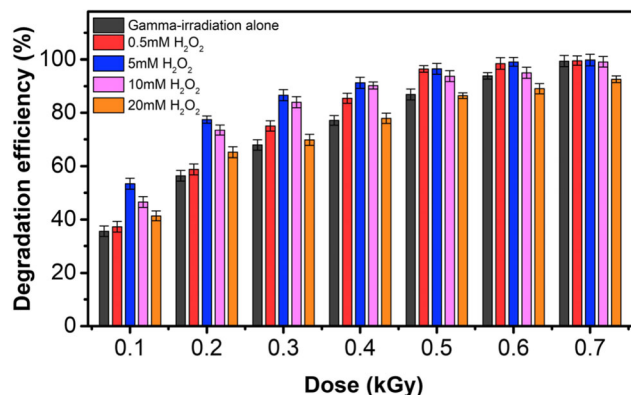


Fig. 5 Effect of H₂O₂ on radiolytic decomposition of ORZ [(ORZ)₀ = 50 mg L⁻¹; pH = 6.5]

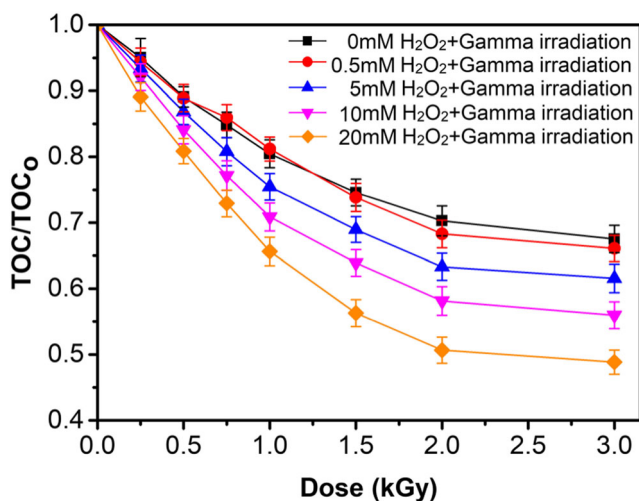


Fig. 6 Effect of absorbed dose and initial H₂O₂ concentration on TOC removal ([ORZ]₀ = 50 mg L⁻¹; [TOC]₀ = 82.5 mg L⁻¹; pH = 6.5)

selectively with ORZ, its decomposition intermediates and eventually leads to the enhanced mineralization. However, at an absorbed dose of 3.0 kGy, organic by-products formed during ORZ decomposition are expected to exhibit remaining TOC in the solutions despite almost complete decomposition of ORZ at 3.0 kGy. Similar results were also obtained in the decomposition of chlorophenols (Hu and Wang 2007), nitrophenol (Yu et al. 2010), sulfamethazine (Liu and Wang 2013) ofloxacin (Changotra et al. 2018), and dyes (Wang et al. 2006) under irradiations.

Statistical analysis

Statistic comparison significant test ($p = 0.05$) using ANOVA (analysis of variance) single factor hypothesis was applied to assess the significant difference between the results available in Table 1. In general, if p value is less than 0.05, the design model is considered to be significant and can be used as statistical predictive model. For all the experiments, the very small p value and high F value indicated that the model was statistically significant and valid (Table S1, supplementary data).

Gaussian calculations

Gaussian 03 Software (Frisch et al. 2003) at density functional theory with B3LYP/6-31G(d) level was considered to optimize the geometry structure of ORZ molecule, which might be used to evaluate the charge distribution of the ORZ molecule through Gaussian calculations. Figure 7 shows the result of charge distribution of ORZ obtained by Gaussian calculation. It was found that C[16] had the highest negative charge (-0.574). Therefore, the strong electrophilic species HO[•] radicals can attack to C[16] atom. As a result, the bond Cl[19]–

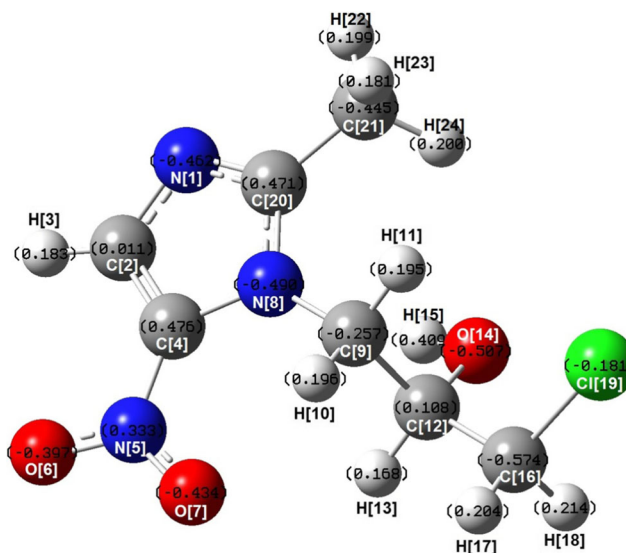


Fig. 7 ORZ molecule structure and its charge distribution

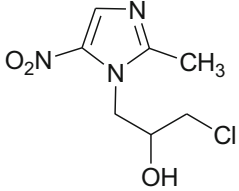
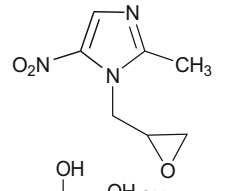
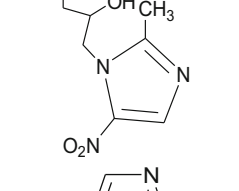
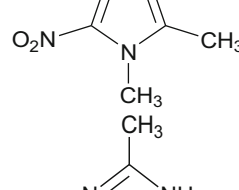
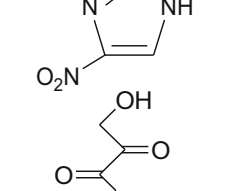
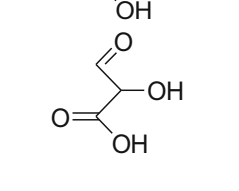
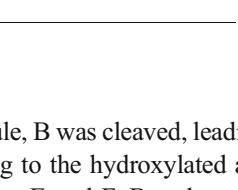
C[16] becomes most susceptible to be cleaved to form new intermediates as also evidenced from product analysis studies in the subsequent section. Thus, we can presume that the gamma-radiolytic decomposition of ORZ is mainly attributed to HO[•] oxidation. In addition, O[14] (-0.507) possess the second higher negative charge, which shows that HO[•] radical can also attack O[14]. Similarly, the bonds of C[21]–H[24], C[12]–C[9], N[1]–C[20], and N[9]–C[8] may be possibly broken due to negative charges. Based on the prediction of Gaussian calculations, we can propose the possible cleavage of bonds of O[14]–C[12], H[24]–C[21], N[9]–C[8], C[20]–N[1], C[9]–C[12], and C[16]–Cl[19] under gamma radiolysis and subsequent formation of some new products.

Reaction mechanism

To confirm the formation of intermediates/products from the gamma radiolytic decomposition of ORZ, the reaction by-products of irradiated solutions were analyzed by LC-QTOF-MS. The radiolytic decomposition products of 50 mg L⁻¹ ORZ at an absorbed dose of 2.0 kGy were identified using LC-QTOF-MS. Six major decomposition by-products were identified, and their retention time as well as molecular structure are listed in Table 2. Based on the obtained results, the removal pathways of gamma-induced radiolytic decomposition of ORZ can be inferred in Fig. 8.

In one instance, HO[•] radicals can react with ORZ to generate intermediate A (ormidazole epoxide), which represents one of the oxidative decomposition products of ORZ as discussed in previous studies (Zhao et al. 2012; Salo et al. 2003). The obtained intermediate is in consistent with the results of Gaussian calculations. The second instance may be the direct decomposition of ORZ under gamma radiolysis.

Table 2 Intermediate compounds during gamma radiolytic decomposition of ORZ

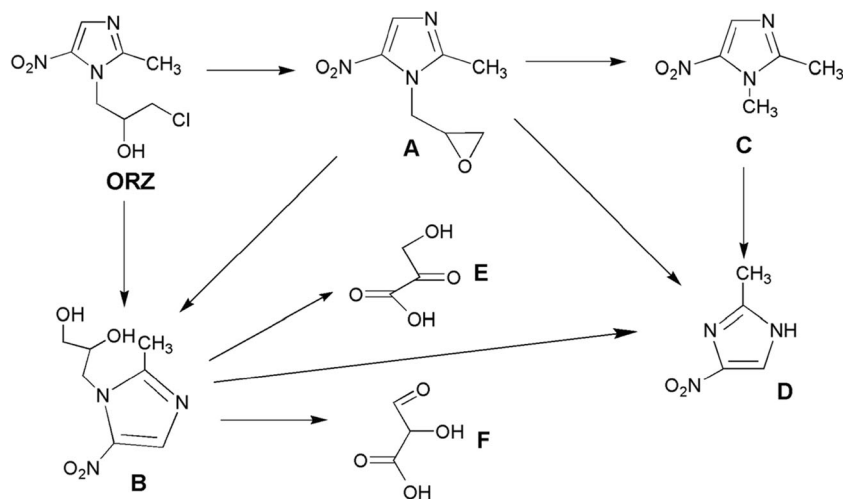
Compound	Retention time (min)	Observed m/z [M+H] ⁺	Calculated m/z [M+H] ⁺	Elemental composition [M+H] ⁺	Proposed structure [M+H] ⁺
ORZ	5.35	221.0019	219.0381	C ₇ H ₁₀ ClN ₃ O ₃	
A	5.12	184.0030	184.06439	C ₇ H ₉ N ₃ O ₃	
B	5.18	201.0030	201.07496	C ₇ H ₁₁ N ₃ O ₄	
C	2.46	142.0294	142.05385	C ₅ H ₇ N ₃ O ₂	
D	3.32	128.0560	128.03818	C ₄ H ₅ N ₃ O ₂	
E	5.12-5.18	104.0521	104.01096	C ₃ H ₄ O ₄	
F	5.12-5.18	104.0521	104.01096	C ₃ H ₄ O ₄	

Further, breaking of C[9]–C[12] bond in amidazole epoxide generates intermediate C (1,2-dimethyl-5-nitroimidazole), which further generates intermediate D (2-methyl-5-nitroimidazole) by demethylation of intermediate C (Salo et al. 2003). In addition, the intermediate D may also be generated by breaking of N[8]–C[9] bond in intermediate A (omidazole epoxide). Further, intermediate B (omidazole glycol) can be generated from ORZ by hydrolytic halogenation of aliphatic halomethyl Cl[19]. In addition to this, intermediate B is expected to be formed from intermediate A by the attack of HO[•] radicals (Salo et al. 2003). Combining with the

optimization results of ORZ molecule, B was cleaved, leading to D and to a moiety corresponding to the hydroxylated aliphatic chain, itself being oxidized to E and F. Based on the intermediate B, the products of E and F could be generated during the gamma radiolysis due to the instability of O[14]–C[12], N[8]–C[9], C[21]–H[24], and N[1]–C[20] bonds.

Therefore, we could attribute the main decomposition mechanism of ORZ during gamma radiolysis to HO[•] radicals oxidation and the direct decomposition of ORZ molecule. In addition, results of LC-QTOF/MS and the Gaussian calculations are able to predict the ORZ decomposition mechanism.

Fig. 8 The main decomposition pathways of ORZ during gamma radiolysis



Toxicity study

The toxicity potential of ORZ and its irradiated solutions (at different absorbed dose) was studied through Standard Kirby-Bauer (disk diffusion) method against clinical isolates of three microbes: *E. coli*, *B. subtilis*, and *P. aeruginosa*. The results indicated that the irradiated as well as un-irradiated ORZ solution (i.e., 50 mg L⁻¹ ORZ concentration) did not showed any toxicity against any of the microbes. Thus, it can be concluded that the parent compound (ORZ) as well as the intermediates produced during gamma radiolytic decomposition of ORZ are non-toxic to the studied microbes. However, as discussed in the “Mineralization study” section, the TOC of the solution significantly decreased upon gamma irradiation and that is most important for the availability of dissolved oxygen in water.

Conclusion

Gamma radiolysis proved to be an effective method to decompose ORZ in the aqueous medium and the decomposition followed pseudo first-order kinetics model. G-(ORZ) increased and dose constant reduced with higher initial concentrations of ORZ. ORZ decomposition efficiency increased in acidic medium when compared to alkaline/neutral medium. Studies with the additives (CO₃²⁻ and *t*-BuOH) revealed that the main pathway of ORZ decomposition was via the HO[•] oxidation. Addition of H₂O₂ resulted in the effective mineralization of ORZ. Gaussian calculations and LC-QTOF-MS analysis demonstrated that radiolytic decomposition of ORZ was mainly controlled by the oxidation of HO[•] radicals and the direct decomposition of ORZ molecules. Thus, the results stimulate to employ gamma radiolysis as a competent and promising wastewater treatment technology for the effective decomposition as well as mineralization of water

contaminants. The treated water can further be recycled in various agricultural fields for irrigation purpose.

Acknowledgements We are thankful to Sophisticated Analytical Instrumentation Facility (SAIF) Lab, Panjab University, Chandigarh for the LC-QTOF-MS facility.

Funding information This research is supported and funded by the Department of Atomic Energy-Board of Research in Nuclear Sciences, Government of India [DAE-BRNS Project No. 35/14/48/BRNS-2014].

Compliance with ethical standards

Conflict of interest The authors declare that they have no conflict of interest.

References

- Andreozzi R, Canterino M, Giudice RL, Marotta R, Pinto G, Pollio A (2006) Lincomycin solar photodegradation, algal toxicity and removal from wastewaters by means of ozonation. *Water Res* 40: 630–638
- Bao H, Gao J, Liu Y, Su Y (2009) A study of biodegradation/ γ -irradiation on the degradation of p-chloronitrobenzene. *Radiat Phys Chem* 78: 1137–1139
- Basfar AA, Khan HM, Al-Shahrani AA, Cooper WJ (2005) Radiation induced decomposition of methyl tert-butyl ether in water in presence of chloroform: kinetic modelling. *Water Res* 39:2085–2095
- Basfar AA, Mohamed KA, Al-Abdul AJ, Al-Shahrani AA (2009) Radiolytic degradation of atrazine aqueous solution containing humic substances. *Ecotoxicol Environ Saf* 72:948–953
- Bojanowska-Czajka A, Drzewicz P, Kozyra C, Nałęcz-Jawecki G, Sawicki J, Szostek B, Trojanowicz M (2006) Radiolytic degradation of herbicide 4-chloro-2-methyl phenoxyacetic acid (MCPA) by γ -radiation for environmental protection. *Ecotoxicol Environ Saf* 65: 265–277
- Borrely SI, Morais AV, Rosa JM, Badaró-Pedroso C, da Conceição Pereira M, Higa MC (2016) Decoloration and detoxification of effluents by ionizing radiation. *Radiat Phys Chem* 124:198–202
- Buxton GV, Greenstock CL, Helman WP, Ross AB (1988) Critical review of rate constants for reactions of hydrated electrons, hydrogen

- atoms and hydroxyl radicals (OH/O^\cdot) in aqueous solution. *J Phys Chem Ref Data* 17:513–886
- Cantwell RE, Hofmann R (2011) Ultraviolet absorption properties of suspended particulate matter in untreated surface waters. *Water Res* 45(3):1322–1328
- Changotra R, Rajput H, Dhir A (2017) Natural soil mediated photo Fenton-like processes in treatment of pharmaceuticals: batch and continuous approach. *Chemosphere* 188:345–353
- Changotra R, Guin JP, Varshney L, Dhir A (2018) Assessment of reaction intermediates of gamma radiation-induced degradation of ofloxacin in aqueous solution. *Chemosphere* 208:606–613
- Changotra R, Varshney L, Paul Guin J, Dhir A (2018a) Performance of hematite particles as an Iron source for the degradation of ornidazole in photo-fenton process. *J Sol-Gel Sci Technol* 85:203–212
- Chen K, Zhou JL (2014) Occurrence and behavior of antibiotics in water and sediments from the Huangpu River, Shanghai, China. *Chemosphere* 95:604–612
- Chu L, Yu S, Wang J (2016) Gamma radiolytic degradation of naphthalene in aqueous solution. *Radiat Phys Chem* 123:97–102
- Dantas RF, Contreras S, Sans C, Esplugas S (2008) Sulfamethoxazole abatement by means of ozonation. *J Hazard Mater* 150:790–794
- Dinh QT, Alliot F, Moreau-Guigon E, Eurin J, Chevreuil M, Labadie P (2011) Measurement of trace levels of antibiotics in river water using on-line enrichment and triple-quadrupole LC–MS/MS. *Talanta* 85:1238–1245
- el mehdi Benacherine M, Debbache N, Ghoul I, Mameri Y (2017) Heterogeneous photoinduced degradation of amoxicillin by goethite under artificial and natural irradiation. *J Photochem Photobiol A Chem* 335:70–77
- Frisch MJ, Trucks GW, Schlegel HB, Scuseria GE, Robb MA, Cheeseman JR (2003) Gaussian 03, Revision B. 04. Gaussian, Inc., Pittsburgh
- Guin JP, Bhardwaj YK, Naik DB, Varshney L (2014) Evaluation of efficiencies of radiolysis, photocatalysis and ozonolysis of modified simulated textile dye waste-water. *RSC Adv* 4:53921–53926
- Guin JP, Naik DB, Bhardwaj YK, Varshney L (2014a) An insight into the effective advanced oxidation process for treatment of simulated textile dye waste water. *RSC Adv* 4:39941–39947
- Guo Z, Dong Q, He D, Zhang C (2012) Gamma radiation for treatment of bisphenol A solution in presence of different additives. *Chem Eng J* 183:10–14
- Guo Z, Zhu S, Zhao Y, Cao H, Liu F (2015) Radiolytic decomposition of ciprofloxacin using γ irradiation in aqueous solution. *Environ Sci Pollut Res* 22:15772–15780
- Guo Z, Guo A, Guo Q, Rui M, Zhao Y, Zhang H, Zhu S (2017) Decomposition of dexamethasone by gamma irradiation: kinetics, degradation mechanisms and impact on algae growth. *Chem Eng J* 307:722–728
- Hapeshi E, Achilleos A, Vasquez MI, Michael C, Xekoukoulotakis NP, Mantzavinos D, Kassinos D (2010) Drugs degrading photocatalytically: kinetics and mechanisms of ofloxacin and atenolol removal on titania suspensions. *Water Res* 44:1737–1746
- Henzler AF, Greskowiak J, Massmann G (2014) Modeling the fate of organic micropollutants during river bank filtration (Berlin, Germany). *J Contam Hydrol* 156:78–92
- Hu J, Wang J (2007) Degradation of chlorophenols in aqueous solution by γ -radiation. *Radiat Phys Chem* 76:1489–1492
- Huang D, Wang Z, Zhang J, Feng J, Zheng Z, Zhang J (2016) Gamma radiolytic degradation of 3,4-dichloroaniline in aqueous solution. *Sep Purif Technol* 170:264–271
- Huie RE, Clifton CL, Neta P (1991) Electron transfer reaction rates and equilibria of the carbonate and sulfate radical anions. *Int J Radiat Appl Instrum Part C Radiat Phys Chem* 38:477–481
- Khan JA, Shah NS, Khan HM (2015) Decomposition of atrazine by ionizing radiation: kinetics, degradation pathways and influence of radical scavengers. *Sep Purif Technol* 156:140–147
- Khatab FI, Ramadan NK, Hegazy MA, Ghoniem NS (2012) Stability-indicating methods for the determination of ornidazole in the presence of its degradate according to ICH guidelines. *Pharm Anal Acta* 3:1000179
- Kim HY, Kim T-H, Cha SM, Yu S (2017) Degradation of sulfamethoxazole by ionizing radiation: identification and characterization of radiolytic products. *Chem Eng J* 313:556–566
- Kostich MS, Batt AL, Lazorchak JM (2014) Concentrations of prioritized pharmaceuticals in effluents from 50 large wastewater treatment plants in the US and implications for risk estimation. *Environ Pollut* 184:354–359
- Kumar A, Xagorarakis I (2010) Pharmaceuticals, personal care products and endocrine-disrupting chemicals in U.S. surface and finished drinking waters: a proposed ranking system. *Sci Total Environ* 408:5972–5989
- Kümmerer K, Al-Ahmad A, Mersch-Sundermann V (2000) Biodegradability of some antibiotics, elimination of the genotoxicity and affection of wastewater bacteria in a simple test. *Chemosphere* 40:701–710
- Le-Minh N, Khan SJ, Drewes JE, Stuetz RM (2010) Fate of antibiotics during municipal water recycling treatment processes. *Water Res* 44:4295–4323
- Liu Y, Wang J (2013) Degradation of sulfamethazine by gamma irradiation in the presence of hydrogen peroxide. *J Hazard Mater* 250–251:99–105
- Liu Q, Luo X, Zheng Z, Zheng B, Zhang J, Zhao Y, Yang X, Wang J, Wang L (2011) Factors that have an effect on degradation of diclofenac in aqueous solution by gamma ray irradiation. *Environ Sci Pollut Res* 18:1243–1252
- Liu N, Wang T, Zheng M et al (2015) Radiation induced degradation of antiepileptic drug primidone in aqueous solution. *Chem Eng J* 270:66–72
- Liu N, Huang W, Li Z, Shao H, Wu M, Lei J, Tang L (2018) Radiolytic decomposition of sulfonamide antibiotics: implications to the kinetics, mechanisms and toxicity. *Sep Purif Technol* 202:259–265
- Magureanu M, Piroi D, Mandache NB, David V, Medvedovici A, Parvulescu VI (2010) Degradation of pharmaceutical compound pentoxifylline in water by non-thermal plasma treatment. *Water Res* 44:3445–3453
- Michael I, Hapeshi E, Michael C, Fatta-Kassinos D (2010) Solar Fenton and solar TiO_2 catalytic treatment of ofloxacin in secondary treated effluents: evaluation of operational and kinetic parameters. *Water Res* 44:5450–5462
- Mohamed KA, Basfar AA, Al-Shahrani AA (2009) Gamma-ray induced degradation of diazinon and atrazine in natural groundwaters. *J Hazard Mater* 166:810–814
- Nam S-W, Jo B-I, Yoon Y, Zoh K-D (2014) Occurrence and removal of selected micropollutants in a water treatment plant. *Chemosphere* 95:156–165
- Panizza M, Dirany A, Sirés I, Haidar M, Oturan N, Oturan MA (2014) Complete mineralization of the antibiotic amoxicillin by electro-Fenton with a BDD anode. *J Appl Electrochem* 44:1327–1335
- Paul J, Naik DB, Bhardwaj YK, Varshney L (2014) Studies on oxidative radiolysis of ibuprofen in presence of potassium persulfate. *Radiat Phys Chem* 100:38–44
- Paul J, Kadam AA, Govindwar SP, Kumar P, Varshney L (2013) An insight into the influence of low dose irradiation pretreatment on the microbial decolouration and degradation of reactive Red-120 dye. *Chemosphere* 90:1348–1358
- Puttaswamy SA, Shubha JP (2009) Kinetics and reactivities of ruthenium (III)- and osmium (VIII)-catalyzed oxidation of ornidazole with chloramine-T in acid and alkaline media: a mechanistic approach. *J Mol Catal A Chem* 310:24–33
- Razavi B, Song W, Cooper WJ, Greaves J, Jeong J (2009) Free-radical-induced oxidative and reductive degradation of fibrates

- pharmaceuticals: kinetic studies and degradation mechanisms. *J Phys Chem A* 113:1287–1294
- Salo JK, Yli-Kauhaluoma J, Salomies H (2003) On the hydrolytic behavior of tinidazole, metronidazole, and ornidazole. *J Pharm Sci* 92: 739–746
- Sánchez-Polo M, López-Peñalver J, Prados-Joya G, Ferro-García MA, Rivera-Utrilla J (2009) Gamma irradiation of pharmaceutical compounds, nitroimidazoles, as a new alternative for water treatment. *Water Res* 43:4028–4036
- Sayed M, Khan JA, Shah LA, Shah NS, Khan HM, Rehman F, Khan AR, Khan AM (2016) Degradation of quinolone antibiotic, norfloxacin, in aqueous solution using gamma-ray irradiation. *Environ Sci Pollut Res* 23:13155–13168
- Schaidler LA, Rudel RA, Ackerman JM, Dunagan SC, Brody JG (2014) Pharmaceuticals, perfluorosurfactants, and other organic wastewater compounds in public drinking water wells in a shallow sand and gravel aquifer. *Sci Total Environ* 468–469:384–393
- Schwartz DE, Jeunet F (1976) Comparative pharmacokinetic studies of ornidazole and metronidazole in man. *Chemotherapy* 22:19–29
- Schwarzenbach RP, Escher BI, Fenner K, Hofstetter TB, Johnson CA, Von Gunten U, Wehrli B (2006) The challenge of micropollutants in aquatic systems. *Science* 313:1072–1077
- Shanmugam G, Sampath S, Selvaraj KK, Larsson DGJ, Ramaswamy BR (2014) Non-steroidal anti-inflammatory drugs in Indian rivers. *Environ Sci Pollut Res* 21:921–931
- Singh P, Mittal R, Sharma GC, Singh S, Singh A (2003) Ornidazole: comprehensive profile. *Profiles Drug Subst Excipients Relat Methodol* 30:123–184
- Solomon WDS, Gowda KV, Selvan PS, Mandal U, Pal TK (2008) HPLC method for quantification of ornidazole in human plasma. *Asian J Chem* 20:4361–4368
- Spinks JWT, Woods RJ (1990) An introduction to radiation chemistry. Wiley, New York
- Tay KS, Madehi N (2015) Ozonation of ofloxacin in water: by-products, degradation pathway and ecotoxicity assessment. *Sci Total Environ* 520:23–31
- Tayo LL, Caparanga AR, Doma BT, Liao C-H (2018) A review on the removal of pharmaceutical and personal care products (PPCPs) using advanced oxidation processes. *J Adv Oxid Technol* 21:196–214
- Tian M, Adams B, Wen J, Asmussen RM, Chen A (2009) Photoelectrochemical oxidation of salicylic acid and salicylaldehyde on titanium dioxide nanotube arrays. *Electrochim Acta* 54:3799–3805
- Wang M, Yang R, Wang W, Shen Z, Bian S, Zhu Z (2006) Radiation-induced decomposition and decoloration of reactive dyes in the presence of H₂O₂. *Radiat Phys Chem* 75:286–291
- Watkinson AJ, Murby EJ, Costanzo SD (2007) Removal of antibiotics in conventional and advanced wastewater treatment: implications for environmental discharge and wastewater recycling. *Water Res* 41: 4164–4176
- Woods RJ, Pikaev AK (1994) Applied radiation chemistry: radiation processing. Wiley
- Yu S, Hu J, Wang J (2010) Gamma radiation-induced degradation of p-nitrophenol (PNP) in the presence of hydrogen peroxide (H₂O₂) in aqueous solution. *J Hazard Mater* 177:1061–1067
- Zhao J, Yao B, He Q, Zhang T (2012) Preparation and properties of visible light responsive Y³⁺ doped Bi₅Nb₃O₁₅ photocatalysts for Ornidazole decomposition. *J Hazard Mater* 229–230:151–158
- Zheng BG, Zheng Z, Zhang JB, Luo XZ, Wang JQ, Liu Q, Wang LH (2011) Degradation of the emerging contaminant ibuprofen in aqueous solution by gamma irradiation. *Desalination* 276:379–385